JOURNAL OF VIROLOGY, June 2005, p. 7629–7640 Vol. 79, No. 12
0022-538X/05/$08.00+0 doi:10.1128/JVI.79.12.7629–7640.2005

Murine Coronavirus Evolution In Vivo: Functional Compensation of a Detrimental Amino Acid Substitution in the Receptor Binding Domain of the Spike Glycoprotein

Sonia Navas-Martin,* Susan T. Hingley,† and Susan R. Weiss

Department of Microbiology, University of Pennsylvania School of Medicine, Philadelphia, Pennsylvania

Received 29 November 2004/Accepted 7 February 2005

Murine coronavirus A59 strain causes mild to moderate hepatitis in mice. We have previously shown that mutants of A59, unable to induce hepatitis, may be selected by persistent infection of primary glial cells in vitro. These in vitro isolated mutants encoded two amino acids substitutions in the spike (S) gene: Q159L lies in the putative receptor binding domain of S, and H716D, within the cleavage signal of S. Here, we show that hepatotropic revertant variants may be selected from these in vitro isolated mutants (Q159L-H716D) by multiple passages in the mouse liver. One of these mutants, hr2, was chosen for more in-depth study based on a more hepatovirulent phenotype. The S gene of hr2 (Q159L-R654H-H716D-E1035D) differed from the in vitro isolates (Q159L-H716D) in only 2 amino acids (R654H and E1035D). Using targeted RNA recombination, we have constructed isogenic recombinant MHV-A59 viruses differing only in these specific amino acids in S (Q159L-R654H-H716D-E1035D). We demonstrate that specific amino acid substitutions within the spike gene of the hr2 isolate determine the ability of the virus to cause lethal hepatitis and replicate to significantly higher titers in the liver compared to wild-type A59. Our results provide compelling evidence of the ability of coronaviruses to rapidly evolve in vivo to highly virulent phenotypes by functional compensation of a detrimental amino acid substitution in the receptor binding domain of the spike glycoprotein.

Coronaviruses comprise a large group of avian and mammalian enveloped, positive sense, polyadenylated RNA viruses that have the largest viral RNA genomes known (49). Mouse hepatitis virus (MHV) is the prototype of group 2 coronaviruses (26). The identification of a new coronavirus as the etiological agent of severe acute respiratory syndrome (SARS) (11, 41) highlights the urgent need to characterize at the molecular level the mechanisms of coronaviruses-induced disease. While the molecular determinants of coronaviruses' pathogenesis remain poorly understood, there is evidence that both host and viral factors do play a role in coronavirus-induced disease (recently reviewed in references 38 and 39). In a defined host genetic background (CB57L/6 mice), murine coronaviruses cause acute and chronic infections in the central nervous system (CNS) and acute self-limited as well as fulminant hepatitis, depending on virus strain (20, 49). MHV-A59 strain is a moderately hepatotropic virus that also causes acute meningoencephalitis and chronic demyelination (32). Using chimeric isogenic A59 recombinant viruses expressing strain-specific spike (S) genes (MHV-2, MHV-JHM, and A59 spikes) we have previously demonstrated that the spike protein of murine coronaviruses is a major determinant of neurovirulence (42), demyelination (9) and hepatotropism (36).

Coronavirus spike protein interacts with receptor and is a major target of neutralizing antibodies (15, 16). Coronavirus spike protein is a class I fusion protein that, depending on virus group, strain and cell type, can be cleaved to different extents into two subunits (6, 10). For example, SARS-CoV as well as group I coronaviruses' spikes (human CoV-229E, porcine transmissible gastroenteritis and respiratory virus (TGEV), feline infectious peritonitis virus (FIPV), among others) lack a proteolytic cleavage sequence BBXBB (B stands for basic residue). This sequence is believed to be the recognition site for cleavage by furin like enzymes (10). This proteolytic cleavage signal (RXR/KR) is however present in many other coronavirus S proteins such as some group II coronaviruses (bovine coronavirus (BCV), and some murine coronaviruses (MHV-JHM, MHV-A59, MHV-3) among others). Murine coronavirus A59 strain S protein is synthesized as a 120-kDa precursor, which is cotranslationally glycosylated to a 150-kDa glycoprotein, and processed to a 180-kDa form during transport from the endoplasmic reticulum through the Golgi complex. Later in maturation, S is cleaved into two 90-kDa noncovalently associated subunits, S1 and S2. S1 contains the receptor binding domain (RBD) as well as a hypervariable region (HVR); while S2 is highly conserved, containing features common to many viral fusion proteins, including two heptad repeat domains (HR1 and HR2) as well as a transmembrane domain (6, 14, 44, 50, 52). These domains are believed to be important in viral entry and in the cell-to-cell fusion process (15).

We have previously described mutants of MHV-A59 isolated from persistently infected primary glial cell cultures (17). These mutants had a fusion-delayed phenotype in vitro and were attenuated in vivo. These phenotypes were associated with two amino acids substitutions in the S protein from two independently derived glial cell variants, called B11 and C12 (17). One substitution, (Q159L) lies in the putative RBD of S, and the second substitution (H716D) within the cleavage signal

* Corresponding author. Mailing address: Department of Microbiology, University of Pennsylvania, School of Medicine, 36th Street and Hamilton Walk, Philadelphia, PA 19104-6076. Phone: 215-898-4672. Fax: 215-573-4858 E-mail: snavas@mail.med.upenn.edu.

† Present address: Department of Pathology, Microbiology and Immunology, Philadelphia College of Osteopathic Medicine, Philadelphia, Pa.

of S (RRAHR). Notably, these in vitro-isolated A59 variants (Q159L-H716D) had an impaired ability to induce hepatitis and replicate in the liver of mice whereas in the brain they replicated to similar titers as wild-type (WT) A59 (23).

Using targeted RNA recombination, we have previously demonstrated that Q159L determined the loss in the ability to induce hepatitis, whereas the H716D cleavage site substitution was associated with the fusion delayed phenotype but not with the lack of hepatotropism of the C12 variant (33). In order to gain a better understanding of the regions within the S gene that may determine the hepatitis phenotype, here we derived hepatotropic revertants of the nonhepatotropic, attenuated, fusion-delayed C12 variant (Q159L-H716D) by in vivo adaptation of C12 through the liver of mice. After 8 in vivo passages of C12 through the livers of C57BL/6 mice, 3 independent virus isolates (hr1, hr2, and hr3) were plaque purified and their phenotypes were confirmed by measuring replication in liver and brain. These in vivo isolated viruses regained the ability to replicate in the liver; subsequently, their spikes genes were sequenced and compared to identify amino acid substitutions that may play a role in determining viral tropism. The amino acid substitutions in hr2 (Q159L-R654H-H716D-E1035D) were selected for additional analysis. Our hypothesis is that one or both of these additional amino acid substitutions (R654H or/and E1035D) are functionally suppressing the detrimental effect of the RBD substitution Q159L, determining a highly hepatotropic phenotype. To test this hypothesis we have generated isogenic recombinant A59 viruses with one or more of the Q159L-R654H-H716D-E1035D substitutions alone or in combination, and examined their ability to produce hepatitis. Surprisingly, neither of the two mutations alone (R654H, E1035D) is associated with the hepatitis revertant phenotype. Our results rather demonstrate that the cleavage signal substitution (H716D) correlates with highly severe hepatitis, which is neutralized by the Q159L mutation, suggesting that the R654H, E1035D substitutions may trigger a conformational change in the hr2 spike protein that overcomes the effects of the RBD substitution Q159L.

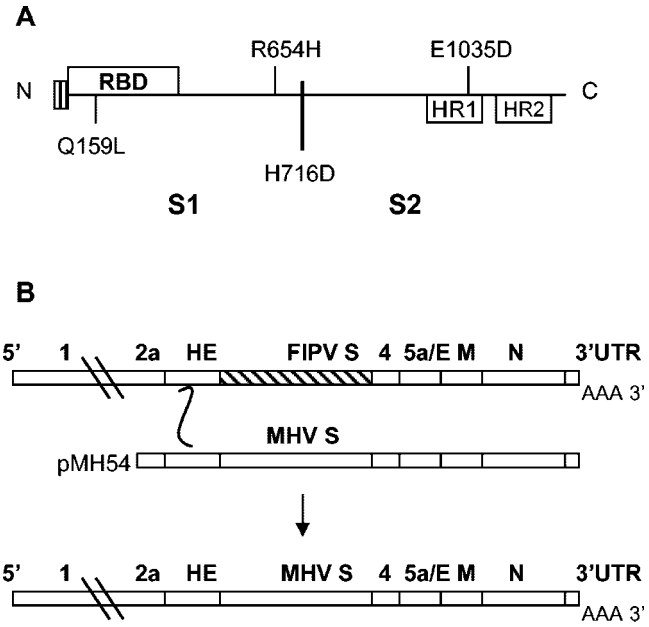

FIG. 1. (A) Schematic of MHV-A59 Spike (S) showing the approximate position of hepatitis revertant hr2 virus amino acid substitutions relative to the receptor binding domain (RBD), cleavage signal, and heptad repeat domains (HR1 and HR2) of S. Spike is cleaved into two 90-kDa noncovalently associated subunits, S1 and S2. S1 contains the receptor binding domain (RBD) and S2 contains amphipathic heptad repeat sequences (HR1 and HR2) important to engage in coiled-coil formation. Q159L lies in the putative RBD of S, H716D within the cleavage signal of S (RRAHR), and E1035D is located in HR1. R654H substitution maps in a region of S in which functional domains have not been yet identified. (B) Scheme of targeted RNA recombination. Feline cells (FCWF) were infected with fMHV, a chimeric recombinant MHV virus expressing the FIPV spike, and then electroporated with pMH54-derived, in vitro transcribed RNA containing the engineered mutations in the spike gene. These infected and eletroporated FCWF cells were overlaid onto murine L2 cells, and recombinants viruses were selected on their ability to infect murine cells (as described in the text).

MATERIALS AND METHODS

Cells and viruses. Murine fibroblast (L2 and 17Cl.1) cells, and *Felis catus* whole-fetus cells (FCWF) cells were maintained in Dulbecco's minimal essential medium (DMEM; Gibco BRL) supplemented with 10% fetal bovine serum (FBS; HyClone Laboratories, Inc., Logan, UT), 1% antibiotic-antimycotic (penicillin-streptomycin-amphotericin B; Gibco), and 10 mM HEPES buffer solution (Gibco).

Wild-type MHV strain A59, C12, hepatitis revertant variants, and recombinant viruses were propagated in mouse 17CL.1 cells; plaque assays and plaque purification of recombinants were carried out in L2 cells. C12 variant is an in vitro isolated MHV strain A59 that we previously isolated and characterized (17, 33). MHV-A59 hepatitis revertant variants were isolated through in vivo adaptation of C12 to the livers of C57BL/6 mice, as described below. The helper virus fMHV used in targeted RNA recombination was provided by Paul Masters (Wadsworth Center for Laboratories and Research, New York Sate Department of Health, Albany, NY) and further propagated in our lab as previously described (30). fMHV is a chimeric MHV-A59 strain virus in which the spike gene of the FIPV was introduced by targeted RNA recombination (30). All MHV-A59 isogenic recombinant viruses differing only in specific amino acid substitutions in the spike protein were generated as described below.

Mice and inoculations. Specific-pathogen-free 4- to 5-week-old male C57BL/6 mice were obtained from the National Cancer Institute (National Institutes of Health). All experiments were performed in containment within a biosafety level 2 animal facility and conducted in accordance with the guidelines of the Institutional Animal Care and Use Committee (IACUC) at the University of Pennsylvania.

Generation of spike transcription vectors. To generate vectors for synthesis of MHV-A59 donor RNAs for targeted RNA recombination with specific amino acid substitutions in the spike gene, plasmid pMH54 (provided by Paul Masters) was modified by site-specific PCR mutagenesis and/or restriction enzyme digestion and ligation of spike gene fragments between pMH54 (wild-type A59) and pMH54-hr2 (hr2 spike), as described below. pMH54 contains the MHV-A59 genome, beginning at codon 28 of the hemagglutinin-esterase (HE) gene to the 3′ end, allowing the manipulation of all ORFs downstream of the HE gene (S, open reading frames [ORFs] 4, 5a, E, M, and nucleocapsid [N] genes) (30) (Fig. 1). In order to generate pMH54-hr2 plasmid, the spike of hr2 isolate (Q159L-R654H-H716D-E1035D) was amplified by reverse transcription (RT)-PCR. Briefly, RNA isolated from cell lysates of hr2-infected L2 cells was reverse transcribed using Superscript II (Invitrogen, Carlsbad, CA) and random primers using 1 μg of total cellular RNA, as described by the manufacturer. A 2-μl aliquot of the cDNA was amplified with a mix of *Tth* DNA polymerase (Roche, Indianapolis, IN) and Vent DNA polymerase (New England Biolabs, Beverly, MA) with primers 5′-cgcgaagcttgaatccTAGGGTATATTGGTGATTTTAGATGTATCCC-3′ and 5′-gcggatccaagtCCtGcAGgGGCTGTGATAGTCAATCCTCATGAGA-3′ using a hot-start long-PCR consisting of one cycle at 94°C for 1 min and at 80°C for 3 min, followed by 30 cycles at 94°C for 30 s, at 50°C for 20 s, at 72°C for 3 min, and at 72°C for 8 min of extension (the lowercase letters in sequence primers correspond to silent modified bases; HindIII-AvrII, and BamHI-SbfI sites are underlined). The resulting PCR product was cloned into TOPO-II vector (Invitrogen) and its sequence was verified by automated se-

TABLE 1. Origin, passage history, and phenotype of MHV-A59 WT, in vitro-isolated C12 variant, and in vivo-isolated hepatitis revertant viruses (hr1, hr2, and hr3)

Virus (nonrecombinant)	Spike genotype	Virus origin	Titer in liver (i.h. inoculation)[a]
MHV-A59	Wild type	Lab strain	6.2
C12	Q159L-H716D	In vitro selection of A59 in murine primary glial cells (persistent nonlytic infection)	4.0
hr1	Q159L-H716D-P839L-E1035D	In vivo adaptation of C12 by eight passages into the livers of mice	5.5
hr2	Q159L-R654H-H716D-E1035D	In vivo adaptation of C12 by eight passages into the livers of mice	7.0
hr3	Q159L-L371S-R654H-H716D-E1035D	In vivo adaptation of C12 by eight passages into the livers of mice	7.4

[a] The ability to replicate in the liver was assessed after i.h. inoculation at 5 days p.i (peak of viral replication). Each titer is the mean from duplicate samples from mice and expressed as $\log_{10}$ PFU/g.

quencing using BigDye Terminator v3.1 cycle sequencing kit (Applied Biosystems, Foster City, CA). The hr2 S gene was then recloned via AvrII (5′-) and SbfI (- 3′) into pMH54 to create pMH54-hr2. pMH54-Q159L was generated by AvrII/DraIII digestion of pMH54-hr2, and subsequent recloning into pMH54. pMH54-E1035D, pMH54-R654H-H716D and pMH54-Q159L-E1035D were generated similarly using the BsrgI-MluI and DraIII-XhoI sites, respectively. pMH54-Q159L-R654H-H716D was constructed using the XhoI and SbfI sites of pMH54-hr2. The R654H substitution was generated by two-step PCR mutagenesis using primers 5′-CTGCTAATTATAAGATTG-3′ and 5′-CTGAGATGCC GTCTGGCAGTCTCG-3′ and primer 5′-CGGCTCTGCTCTATCaTAATA-AATTGTAGCTAT-3′ (a silent mutation to generate the R654H substitution is underlined); a DraIII-XhoI fragment containing the R654H substitution was subsequently cloned into pMH54 and pMH54-Q159L to generate pMH54-R654H and pMH54-Q159L-R654H, respectively. pMH54-R654H-E1035D and pMH54-Q159L-R654H-E1035D were generated by subcloning of a BsrgI-MluI fragment containing the E1035D substitution into pMH54-R654H and pMH54-Q159L, respectively. pMH54-H716D was constructed as previously described by PCR mutagenesis (24). pMH54-Q159L-H716D-E1035D was generated by DraIII-XhoI digestion of pMH54-H716D, and subcloning into pMH54-Q159L-E1035D. Sequence and restriction analysis was performed using Macvector (Accelrys, San Diego, CA).

Targeted RNA recombination. Targeted RNA recombination was carried out between a interspecies chimeric helper fMHV virus (30) and pMH54-derived, in vitro-transcribed RNA containing the engineered mutations in the spike gene, as well as wild-type A59 spike. Briefly, feline cells (FCWF) were infected with fMHV at 0.1 PFU per cell; after 4 h at 37°C, infected cells were gently trypsinized with trypsin (Gibco) diluted at a ratio of 1:8 in phosphate-buffered saline (PBS; Gibco), and electroporated with donor capped RNA transcribed from pMH54 (A59 wild-type spike), and pMH54-mutant spikes. In vitro RNA transcription was performed using mMESSAGE mMACHINE T7 kit (Ambion, Inc., Austin, TX). Infected and transfected feline FCWF cells were overlaid onto murine L2 cells and recombinants were selected on their ability to infect murine cells, as previously described (30). Recombinant viruses were plaque-purified twice and sequenced as described above. At least two recombinant viruses, independently derived from each S construct, were plaque purified and propagated in 17 Cl.1 cells. Virus stocks were kept at −80°C until used.

Assessment of virus growth in tissue culture. L2 cells were infected with virus at a multiplicity of 1 PFU per cell and incubated for 1 h at 37°C. Subsequently, the cells were washed four times to remove residual unbound virus. Supernatants and cells were harvested at various times after infection for virus titration by plaque assay, as previously described (37). Infectious virus in 1:10 serial dilutions of both cell-associated and released virus from in vitro infected L2 cells, was prepared using DMEM–2% FBS. Virus concentrations were determined as PFU/ml.

Viral virulence. Mice were inoculated intracranially with 10-fold serial dilutions of virus, five mice per dilution. Mice were monitored daily for survival and signs of disease for 21 days after inoculation. Fifty percent lethal dose (LD_{50}) values were calculated using the method of Reed and Muench (43). All assays were performed in at least two independent experiments.

Assessment of viral load in mice. At various times after inoculation, mice were sacrificed and livers, and in some cases brains, were harvested. Organs were weighed, homogenized and stored frozen (−80°C) until titered for virus. Virus titers were determined by plaque assay on L2 cell monolayers, as previously described (35). Viral load was determined as PFU per gram of tissue (PFU/g).

Liver histopathology and immunohistochemical staining for MHV antigen. Livers were harvested from infected mice on day 5 postinfection (p.i.), fixed in 10% buffered formalin (Histochoice; Fisher Scientific, Pittsburgh, PA) and embedded in paraffin. Sections of liver were stained with hemotoxylin and eosin (H&E) and examined for morphological evidence of hepatic inflammation and necrosis. Hepatitis was scored as minimal changes (1), mild (2), moderate (3) and severe (4) as previously described (4, 37). Viral antigen was detected using anti-N monoclonal antibody (MAb) 1.16.1 (provided by J. Leibowitz, Texas A&M University) using avidin-horseradish peroxidase complex (ABC) technique (VECTOR, Burlingame, CA) with disaminobenzene chromogen (VECTOR) as previously described (37).

RESULTS

Isolation of hepatotropic revertant viruses from the liver of mice. To assess the role of specific amino acid substitutions of the spike protein in murine coronavirus induced-hepatitis we performed experiments aimed to isolate hepatotropic revertants of a nonhepatototropic MHV-A59 variant called C12. C12 was isolated from persistently infected primary murine glial cell cultures at week 18 postinfection (17); we have previously characterized C12 in vitro as well as in vivo (17, 33). Notably, the ability of C12 to replicate in the liver and induce hepatitis was eliminated and correlated with one amino acid substitution in the RBD of the spike (Q159L), whereas H716D in the cleavage signal of S was associated with a fusion delayed phenotype (33). Here, we derived hepatotropic revertant viruses of C12 by serial passage in mice until hepatitis was observed (passage 8). To avoid infection of the CNS, mice were directly inoculated in the liver and sacrificed at day 4 postinfection. Revertants were plaque purified three times from a liver homogenate of a mouse infected with virus obtained after eight in vivo passages of C12 through the livers of C57BL/6 mice. Three isolates (hr1, hr2, and hr3) were characterized for their ability to replicate in the liver and in the brain after intracranial (i.c.) and intrahepatic (i.h.) inoculations. These isolates demonstrated varying levels of infectious virus in the liver (Table 1), whereas viral load in the brain was similar to WT A59 (data not shown). We next sequenced the S genes of these in vivo isolated variants and compared them to the S genes of WT A59 and C12 variant (Table 1). Notably, all 3-h viruses retained the mutations present in the C12 spike gene (Q159L and H716D), and differed from C12 at amino

TABLE 2. Virulence and hepatitis phenotypes of recombinant viruses after i.c and i.h. inoculations

Virus	Log_{10} LD_{50}		Phenotype Hepatitis	
	Intracranial	Intrahepatic	Intracranial	Intrahepatic
RA59 (wild type)[a]	3.8	[b]	Mild to moderate	[b]
Q159L-H716D (C12)[a]	6.0	[b]	None to minimal	[b]
Q159L-R654H-H716D-1035D (hr2)[a]	1.2	[b]	Severe (lethal)	[b]
Q159L-R654H-H716D	3.8	[b]	Moderate to severe	[b]
Q159L-H716D-E1035D	4.0	[b]	Mild to moderate	[b]
Q159L-R654H-E1035D	4.9	[b]	Mild to moderate	[b]
Q159L-E1035D	4.9	[b]	Mild to moderate	[b]
R654H-E1035D	3.7	[b]	Mild to moderate	[b]
Q159L-R654H	6.1	[b]	None to minimal	[b]
R654H-H716D	1.5	[b]	Severe (lethal)	[b]
Q159L	6.1	[b]	None to minimal	[b]
R654H	3.5	[b]	Mild to moderate	[b]
E1035D	4.5	[b]	Mild to moderate	[b]
H716D	3.6	1.2	Mild to moderate	Severe (lethal)

[a] These recombinant viruses had the same spike sequences as the natural viruses listed in parentheses.
[b] Same values as after i.c. inoculation. After i.h. inoculation, only recombinant virus H716D showed a different virulence value.

acid 1035 (E1035D). In addition, isolates hr2 and hr3 contained a conservative arginine to histidine at position (R654H); a serine for phenylalanine substitution at amino acid residue 371 (S371F) was also observed in hr3. Isolate hr1 had a unique proline to leucine substitution in 839 residue (P839L) (Table 1). Hr2 and hr3 isolates exhibited similar high viral load in the liver, and their spikes differ in only 1 amino acid (hr2, Q159L-R654H-H716D-E1035D; hr3, Q159L-S371F-R654H-H716D-E1035D). Since the mutations present in hr2 spike are the minimal sequence associated to the hepatotropism reversion, we selected hr2 isolate for additional analysis. The positions of these amino acid substitutions relative to the S domains are schematically shown in Fig. 1A.

In order to determine the phenotypes resulting from various combinations of mutations identified in the hr viruses, we constructed isogenic recombinant viruses (all in the A59 background) differing only in specific amino acids of the S gene (Q159L-R654H-H716D-E1035D) (Table 2). Two independent recombinants of each construct were assessed for their ability to replicate in the liver and cause hepatitis after i.c. and i.h. inoculations.

Time course of released and cell-associated virus. We first analyzed whether the spike from the highly hepatotropic hr2 (Q159L-R654D-H716D-E1035D) or any of the specific amino acid substitutions (either alone or in combination) conferred any difference in kinetics of virus production in murine fibroblast L2 cells compared to the A59 wild type (Fig. 2). Cells were infected at 1.0 multiplicity of infection (MOI). and the time course of released and cell-associated virus production was evaluated as previously described (37). Interestingly, we found that cell associated levels (a measure of intracellular virus) of hr2 virus were higher than those observed for the wild-type recombinant RA59 ($P < 0.05$) (Fig. 2B), and in contrast to the wild type, the peak of hr2 released virus was delayed 12 h (peaking at 24 h p.i.) (Fig. 2A). This phenomena is probably a result of the fusion-delayed, less fusogenic phenotype induced by H716D mutation, (a less cytopathic virus might accumulate to higher titers during an infection). Overall, considering both released and cell-associated kinetics, viruses lacking the H716D (that is, with a wild-type cleavage signal) exhibited a similar WT A59 replicating phenotype (Fig. 2A and B). All viruses expressing the cleavage signal substitution (H716D) had a delayed fusion phenotype compared to A59 (data not shown). However, they exhibited various in vitro replication patterns (Fig. 2C). Whereas some recombinants (Q159L-H716D-E1035D) and (Q159L-R654D-H716D) displayed similar replication and release kinetics as hr2, R654D-H716D and H716D viruses exhibited delayed release and in the case of R654D-H716D delayed cell-associated kinetics as well compared to WT or hr2 (Fig. 2C and D). Remarkably, the Q159L amino acid substitution that maps in the putative receptor binding domain (RBD) of the spike (52), previously found by our lab to be associated with impaired replication in the liver (34), did not alter the in vitro phenotype compared to WT A59.

Virulence after intracranial and intrahepatic inoculation. In order to define the role of the hr2 spike amino acid substitutions in virulence, we performed virulence assays measuring LD_{50} by both i.c. and i.h. inoculations of 4-week-old male C57BL/6 mice. We have previously demonstrated that after i.c. inoculation, MHV exhibited the capacity to infect the liver and cause hepatitis (31). In contrast, hepatitis can be experimentally isolated from CNS disease by direct virus inoculation into the liver of mice (23); thus, hepatitis phenotype may be dependent on the route of inoculation. We first assayed virulence by i.c. inoculation (Table 2). Recombinants expressing the hr2 spike (Q159L-R654H-H716D-E1035D) were as virulent (log_{10} LD_{50} = 1.2) as the hr2 nonrecombinant virus (data not shown), demonstrating that the hr2 phenotype was determined by the spike gene. We next systematically assessed the contribution of each amino acid substitution to the virulence of hr2. When E1035D, R654H, and H716D were individually corrected in the context of the hr2 spike, the resulting recombinant viruses exhibited virulence values of 3.8, 4.0, and 4.9 (log_{10} LD_{50}),

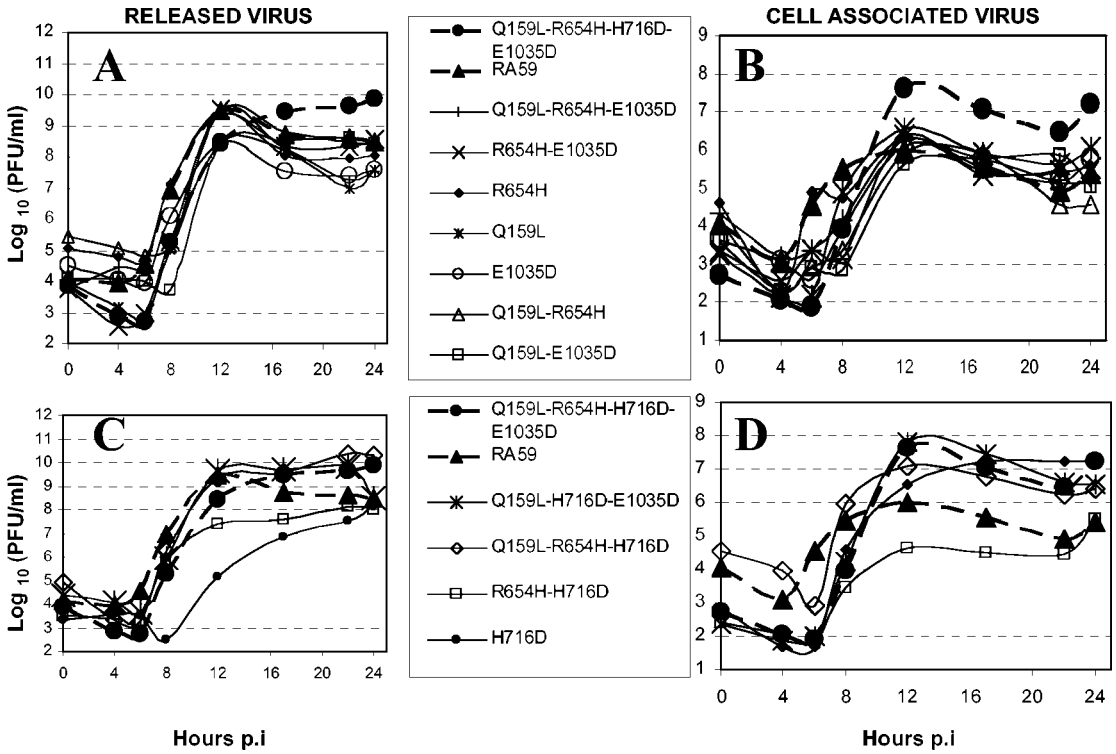

FIG. 2. Time course of released (A and C) and cell-associated virus (B and D) production in L2 cells cultures. Replication kinetics of viruses with a WT cleavage site are shown in A and B, whereas viruses with the H716D amino acid substitution are depicted in C and D. Released and cell-associated kinetics of recombinant RA59 and Q159L-R654H-H716D-E1035D viruses are shown in all panels (A through D). The C12 isolate (Q159L-H716D) has been previously studied in vitro (17); C12 exhibits released and cell associated kinetics similar to hr2 virus (data not shown). L2 cells were infected in duplicate with recombinant viruses at a multiplicity of infection of 1 PFU/cell. The data shown represent the mean titer of duplicate samples. Two independent recombinant viruses were analyzed. At indicated times, virus titers were determined in cells and culture supernatants by plaque assay in L2 cells.

respectively (Table 2). These results suggested that both the R654H and E1035D substitutions contributed to the increased virulence of the hr2 spike, with R654H being more dominant than E1035D; furthermore, these data suggest that the cleavage signal substitution H716D, may play a major role in virulence. Interestingly, whereas R654H alone was incapable of overcoming the receptor binding domain Q159L substitution (Q159L-R654H; $\log_{10}$ LD_{50} = 6.1), E1035D seemed to contribute to both virulence and hepatitis in the presence of Q159L (Q159L-E1035D, $\log_{10}$ LD_{50} = 4.9) (discussed below). The R654H substitution individually did not affect virulence compared to WT A59 virus, whereas E1035D seemed to contribute to attenuation $\log_{10}$ LD_{50} = 4.5. The R654H-H716D virus was as virulent as hr2 (parental and recombinant) ($\log_{10}$ LD_{50} = 1.2 and 1.5, respectively) and also induced lethal hepatitis (further discussed below). Surprisingly, although the H716D virus had WT virulence after intracranial inoculation ($\log_{10}$ LD_{50} = 3.6), a highly virulent phenotype was observed after intrahepatic inoculation ($\log_{10}$ LD_{50} = 1.5). The reason for this difference is not clear. This difference is intriguing, as no differences were observed between i.c. and i.h. inoculations with any of the other viruses (Table 2).

In vivo replication in liver and brain after intrahepatic and intracranial virus inoculation. We next assess whether hr2 (parental, nonrecombinant, as well as two independent isogenic recombinants (Rhr2-A, Rhr2-B)) exhibited differences in viral levels in liver and brain compared to A59 as well as to highly hepatotropic viruses previously described by our lab (MHV-2 strain and recombinant Penn98-1) (9) (Fig. 3). We first infected mice with 500 PFU of virus inoculated directly into the liver as previously described (36) and mice were sacrificed at days 1, 3, 5, and 7 p.i. This dose was used as standard because it is the minimum amount of A59 virus required to induce a wild-type hepatitis (36). Our results demonstrated that isogenic A59 recombinant viruses expressing the hr2 spike (Q159L-R654D-H716D-E1035D) (Rhr2-A, Rhr2-B) replicated to similar level as the parental non-recombinant hr2 and to significantly higher titers than RA59, MHV-2 strain, and a recombinant A59 virus expressing the spike of MHV-2 (Penn98-1) (9, 36) ($P < 0.05$) (Fig. 3A). MHV-2 and Penn98-1 were used as controls as prototypes of viruses with enhanced ability to replicate in the liver and induce hepatitis (36). In contrast, recombinant virus expressing the RBD mutation (Q159L) replicate to a minimal level in the liver ($P < 0.05$), confirming previous results (33). In order to assess whether hr2 viruses are able to replicate in the liver and the brain after i.c. inoculation to the high titers observed following i.h. inoculation, we inoculated 500 PFU of each virus directly into the brain (i.c.) (Fig. 3B and C). Similar results were obtained after i.c. inoculation: hr2, Rhr2-A, and Rhr-2B titers in liver were as high as those obtained after i.h. inoculation, and significantly higher compared to RA59 and Penn98-1 ($P < 0.05$), while

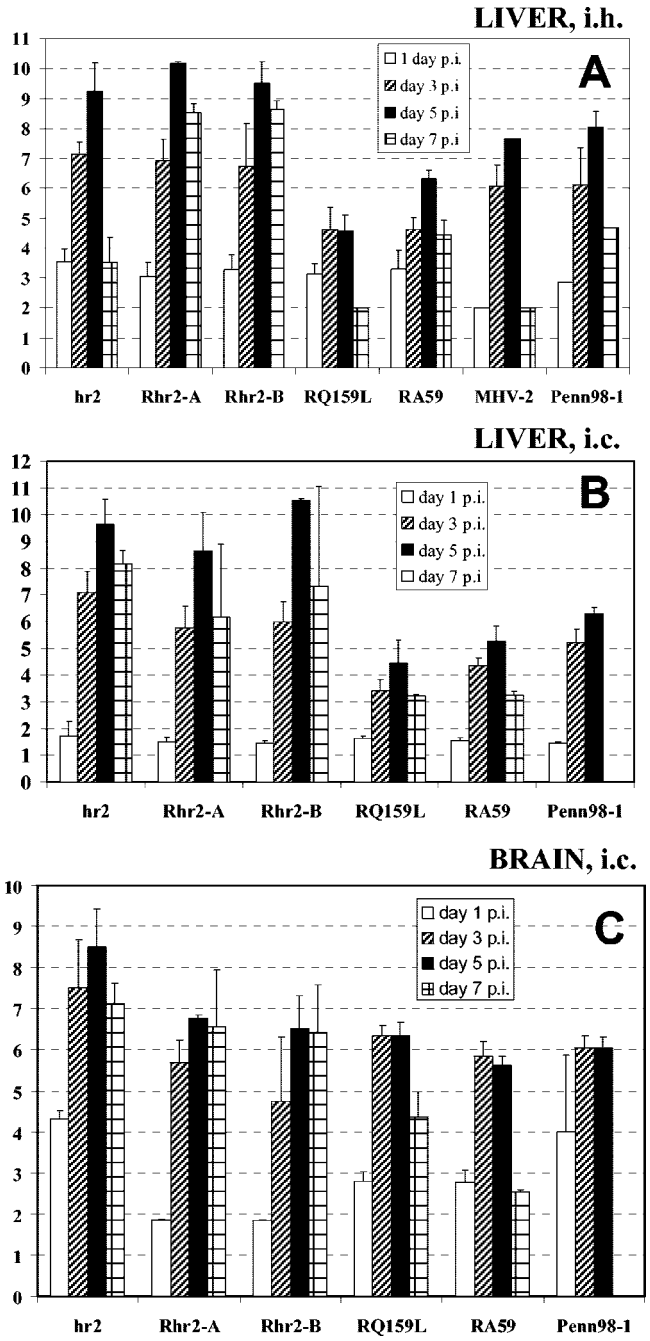

FIG. 3. (A) Viral load in liver of C57BL/6 mice at 1, 3, 5, and 7 days p.i. after i.h. inoculation with 500 PFU of parental hr2 virus as well as recombinant viruses Rhr2-A, Rhr2-B, Q159L, and RA59. The highly hepatotropic MHV-2 (parental virus) and a recombinant A59 expressing the spike of MHV-2 (Penn98-1) were used as controls. Viral titers were determined by plaque assay and are presented as $\log_{10}$ PFU/g of liver. Errors bars represents logarithmic standard deviation. The limit of detection was 200 PFU/g of liver. Five mice per day per virus were examined. Viruses expressing the hr2 spike (hr2 parental, and recombinants Rhr2-A, Rhr2-B) exhibited significant higher viral load in the liver of mice ($P < 0.05$). Viral load in liver (B), and brain (C) at 1, 3, 5, and 7 days p.i. from mice inoculated intracranially with 500 PFU of the above viruses. Parental and recombinant hr2 viruses exhibited higher viral titers in liver (B) than in brain (C) after i.c. inoculation ($P < 0.05$). No significant differences in viral titers among viruses were observed in the brain (C).

Q159L recombinant virus titers were significantly lower ($P < 0.05$). Of note, virus titers in brain were similar among all viruses (hr2 parental, and recombinants Rhr2-A and Rhr2-B, Q159L, RA59, and Penn98-1) and no significant differences were observed (Fig. 3C). This finding suggests that more extensive replication observed with hr2 is specific for the liver. In addition, after i.c. inoculation the Q159L recombinant virus replicated in the brain to levels similar to A59 (Fig. 3C), demonstrating that although Q159L virus is not able to replicate efficiently in the liver, it has a wild-type A59 phenotype in the brain (33, 34).

Overall, these results suggested the following: (i) the highly virulent phenotype of hr2 correlates with higher viral load in liver but not in brain, and (ii) this virulent hepatitis revertant phenotype is determined by the spike gene, demonstrated using isogenic recombinant viruses having an A59 background and differing only in the spike gene (Rhr2-A and -B). These findings prompted us to define the specific amino acid substitutions within the spike gene of hr2 (Q159L-R654H-H716D-E1035D) that determine it highly hepatovirulent phenotype.

H716D substitution is necessary and sufficient to induce high viral loads in the liver and severe hepatitis. Figure 4 shows viral replication titers in the liver and histopathological analysis (Table 3) at day 5 p.i. after direct inoculation into the liver with recombinant viruses depicted in Table 2. Because the C12 isolate (Q159L-H716D) did not induce hepatitis and replicated to a minimal extent in the liver, in contrast to the hr2 mutant Q159L-R654H-H716D-E1035D, it was reasonable to argue that either of the substitutions (R654H or E1035D) that appeared in hr2 spike might be responsible for the highly hepatotropic hr2 phenotype. However, our data demonstrated that R654H and E1035D substitutions, when expressed by recombinant viruses either in combination (R654H-E1035D) or alone (R654H and E1035D) exhibited a WT A59 phenotype in the liver. Furthermore, R654H or E1035D substitutions, alone or together, were not determinants for severe hepatitis (R654H-E1035D, R654H and E1035D viruses were similar to RA59), although they did play a role in the context of the hr2 spike. Interestingly, R654H seemed to play a more dominant role than E1035D in the presence of the two C12 mutations (Q159L-R654H-H716D compared to Q159L-H716D-E1035D, $P < 0.05$). We also noted that H716D correlated with increased liver titers in mice infected with recombinants expressing all combinations of amino acid substitutions except when paired with Q159L, as occurred in the original C12 virus. In fact, the RBD mutation (Q159L) is dominant over both the cleavage site (H716D) mutation (Q159L-H716D compared to H716D virus) and R654H (Q159L-R654H compared to R654H). As seen in Fig. 4A, the Q159L-R654H-H716D virus could partially reverse the attenuating affects of Q159L. This virus exhibited similar high viral load compared to hr2, whereas it had an intermediate hepatitis phenotype between A59 and hr2 viruses (Table 3). This finding demonstrates that the lack of hepatotropism caused by the Q159L mutation is somewhat overcome with R654H-H716D substitutions in combination, but neither amino acid substitution alone was sufficient to induce lethal hepatitis. Finally, the E1035D substitution eliminates the Q159L phenotype, changing the nonhepatotropic Q159L phenotype to a WT A59 phenotype. This effect was observed in viruses Q159L-R654H-E1035D,

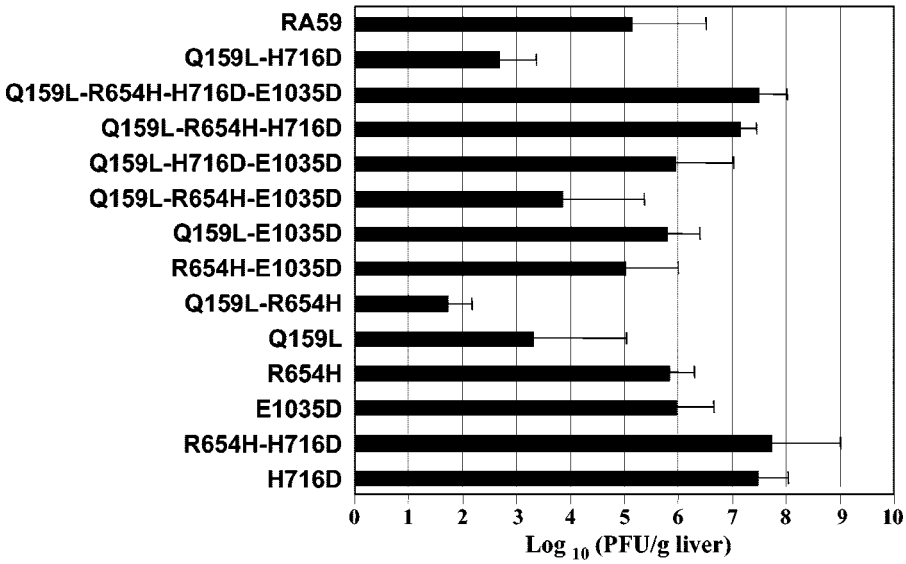

FIG. 4. Viral load in liver of C57BL/6 mice at 5 day p.i. after intrahepatic inoculation with 500 PFU of recombinant viruses RA59, Q159L-H716D, Q159L-R654H-H716D-E1035D, Q159L-R654H-H716D, Q159L-H716D-E1035D, Q159L-R654H-E1035D, Q159L-E1035D, R654H-E1035D, Q159L-R654H, R654H-H716D, Q159L, R654H, E1035D, and H716D. Viral titers were determined by plaque assay and are presented as $\log_{10}$ PFU/g of liver. The limit of detection was 200 PFU/g of liver. Ten mice were examined per virus, and two independent recombinant viruses were evaluated (only results from one independent recombinant per virus are shown).

Q159L-H716D-E1035D, and Q159L-E1035D (compared to Q159L-R654H, Q159L-H716D, and Q159L, respectively).

The presence of the cleavage signal substitution H716D alone, as well as in the presence of R654H (R654H- H716D virus), and in the context of the hr2 spike (Q159L-R654H-H716D-E1035D) correlated with higher viral load in the liver and severe hepatitis. Interestingly, we have observed a lack of correlation between the virulence of H716D virus after i.c. and i.h. inoculations ($\log_{10}$ LD_{50} = 3.6 versus 1.5, respectively) (Table 2), suggesting that H716D phenotype was dependent on the route of inoculation. Figure 5A shows survival curves after i.c. and i.h inoculations with 100 PFU of H716D virus. After direct inoculation into the liver, H716D virus caused 100%

TABLE 3. Viral-induced histopathology in the liver[a]

Virus	Normal	Minimal	Mild	Moderate	Severe
RA59 (wild type)		20	20	60	
Q159L-H716D (C12)	60	40			
Q159L-R654H-H716D-1035D (hr2)					100
H716D				20	80
R654H-H716D				40	60
Q159L-R654H-H716D			40	60	
Q159L-H716D-E1035D			20	20	60
Q159L-E1035D		20	60	20	
R654H		20	40	40	
Q159L-R654H-E1035D	20	20	40	20	
R654H-E1035D		20	40	40	
E1035D		20	40	40	
Q159L-R654H	40	60			
Q159L	40	60			

[a] Viral-induced pathology in the liver was scored as none, minimal, mild, moderate, or severe hepatitis as described in the text. The results are shown as percentages of mice exhibiting none, minimal, mild, moderate, or severe hepatitis.

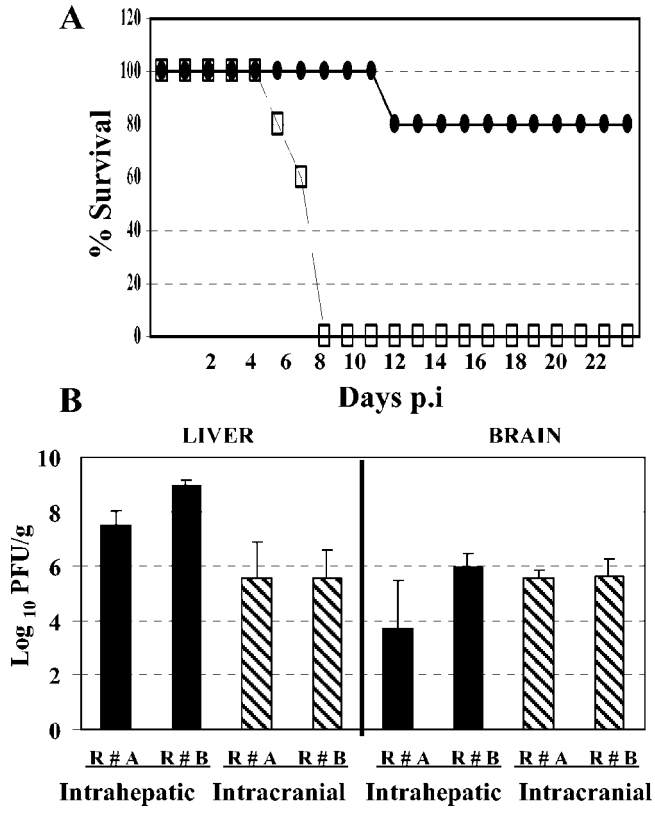

FIG. 5. (A) Susceptibility of C57BL/6 mice to recombinant H716D virus infection after i.c. (●), as well as i.h. (□) inoculations. Survival curves were determined as described in the text. (B) Viral load in liver and brain of mice inoculated after i.h and. i.c. inoculations with two independent recombinant H716D viruses (R# A, R# B).

mortality by day 8 p.i. In contrast, 80% mice recovered from infection after i.c. inoculation, and mortality (20%) was delayed by day 12 p.i. After i.c. inoculation, viral load of H716D virus in the liver was significantly lower ($P < 0.05$), compared to load after direct inoculation into the liver (Fig. 5B). In the brain, intracranial inoculation of H716D virus caused a WT A59 phenotype. Interestingly, infectious virus was recovered from the brains of i.h. inoculated mice (Fig. 5B).

Immunohistochemical analysis revealed enhanced virus spread in liver associated with H716D substitution alone, in the presence of R654H, and in the context of the hr2 spike. We next examined whether there were differences in localization of viral antigen that could be associated with specific sequences in the spike gene of hr2 (Q159L-R654H-H716D-E1035D) (Fig. 6). Livers sections from mice inoculated i.h. with recombinant viruses listed in Table 2 were stained for MHV antigen using a MAb against the nucleocapsid protein of A59 as previously described (36). The time point of 5 days p.i. was chosen for this analysis since this is the peak of virus replication in the liver (36). Overall, no differences in cell tropism were found. Viral antigen colocalized mainly with areas of necrosis and/or inflammation and occasionally with individual hepatocytes and spaces of Disse (consisting with Kupfer and/or endothelial cells). However, we found dramatic differences in the amount of necrosis and virus spread among the various recombinant viruses. These differences defined three phenotypes: minimal, moderate, and severe. Minimal changes were characterized by scattered inflammatory foci with occasional spotty necrosis associated with individual viral-stained hepatocytes. This level of hepatitis was observed with Q159L, Q159L-R654H, and Q159L-H716D viruses. Moderate, A59-like hepatitis, was characterized by multiple foci of hepatocellular necrosis separated by areas of normal parenchyma. Moderate hepatitis was observed for recombinant viruses RA59, E1035D, R654H, R654H-E1035D, Q159L-E1035D, Q159L-R654H-E1035D, and Q159L-H716D-E1035D. Severe hepatitis, with bridging necrosis and extensive, confluent virus spread, was observed in livers from mice infected with both hr2 parental and recombinant (Q159L-R654H-H716D-E1035D) viruses, as well as R654H-H716D, and H716D viruses. Interestingly, Q159L-R654H-H716D exhibited noticeable areas of viral antigen staining, however, the extent of labeling was less prominent than for the hr2 phenotype.

DISCUSSION

In this study, we have derived hepatotropic revertant mutants of a non-hepatotropic, in vitro-isolated A59 variant (C12) by in vivo adaptation of C12 to replicate in the liver of C57BL/6 mice. We have shown that viruses isolated after eight in vivo passages in mice regained the ability to replicate in the liver and induce hepatitis. Of these variants, hr1 had an A59-like phenotype. In contrast, hr2 and hr3 exhibited a more hepatovirulent phenotype than the A59 WT. Hr2 and hr3 spikes differed in only one amino acid (L371S, present only in hr3) (Table 1), although both exhibited similar high viral titers in the liver. Thus, we selected hr2 as the prototype revertant isolate for in depth study. The hr2 isolate exhibited significantly higher viral load and enhanced virus spread in the liver, whereas in the brain, the hr2 phenotype was similar to WT A59. The spike gene of this in vivo isolated hr variant (Q159L-R654H-H716D-E1035D) differed from the in vitro isolates (Q159L-H716D) in only two amino acids (R654H and E1035D). Using targeted RNA recombination we first demonstrated that the spike gene of the hepatitis revertant isolate determines the ability of the virus to cause lethal hepatitis. To more closely define the contributions of each particular amino acids of the hr2 spike protein in the induction of lethal hepatitis, we next systematically generated isogenic recombinant viruses differing only in these specific amino acids in S (Q159L-R654H-H716D-E1035D).

We have previously demonstrated (33) and confirmed in this study, that the RBD Q159L substitution alone is sufficient to abolish hepatitis and is associated with minimal viral loads in the liver. Surprisingly, here we found that neither the R654H nor the E1035D substitution, alone or in combination, determine the hypervirulent hepatitis revertant phenotype. Our findings rather suggest that the R654H and E1035D substitutions may trigger a conformational change in S protein that overcomes the detrimental effects of the RBD substitution Q159L. This data is surprising because both changes (R654H and E1035D) are conservative, although R and H amino acids have very different shapes. It is interesting to note that in the context of the RBD Q159L substitution, neither the cleavage signal (H716D) nor R654H substitutions alone were able to compensate for the lack of hepatotropism determined by Q159L. However, recombinant viruses expressing the spike Q159L-E1035D induced a WT A59-like phenotype, demonstrating that the E1035D substitution may overcome the lack of hepatotropism of Q159L, albeit E1035D alone does not confer lethal hepatitis. The revertant hepatotropic phenotype associated with the E1035D amino acid substitution was also observed in the context of the nonhepatotropic Q159L-R654H, and Q159L-H716D spikes since recombinant viruses Q159L-R654H-E1035D and Q159L-H716D-E1035D induced a WT A59-like phenotype. Same site revertants L159Q were never isolated. On the contrary, viruses with the four mutations were selected in vivo for rather than a wild-type virus in which the Q159L mutation alone had been corrected.

Notably, our results demonstrate that the cleavage signal substitution alone (H716D) or in the context of the R654H substitution (R654H-H716D) correlates with increased virus load and spread in the liver, inducing lethal hepatitis to the same extent as the hr2 isolate (Q159L-R654H-H716D-E1035D). It must be emphasized that hr2, and R654H-H716D viruses were hypervirulent irrespective of the site of inoculation (i.c. or i.h.). In contrast, recombinant H716D viruses induced lethal hepatitis only after direct inoculation in the liver, causing a WT A59-like phenotype after i.c. inoculation. This finding was confirmed in multiple independent experiments using two independent recombinant H716D viruses, suggesting that the cleavage site substitution H716D may interfere with the spread of the virus from the brain to the liver. We have previously observed this phenomena with some other A59 in vitro isolates (23). The mechanisms of coronavirus trafficking between organs of a single infected host have not yet been investigated. One possible explanation for the differences in pathogenesis induced by recombinant H716D viruses after i.c and i.h. inoculations is that the stability of the virus in blood may be impaired due to factors yet to be defined. We have not

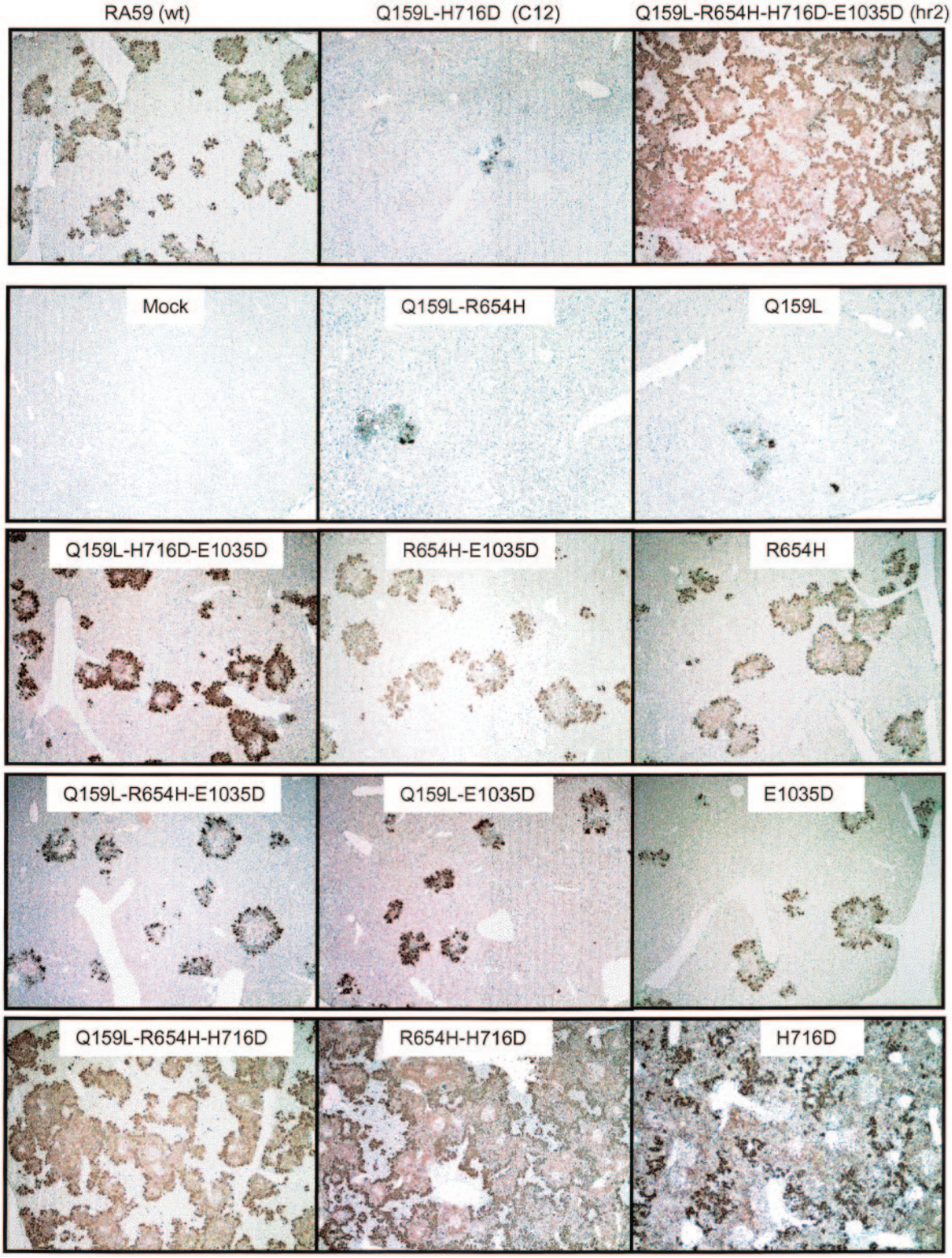

FIG. 6. Immunohistochemistry of liver sections of C57BL/6 mice infected with the recombinant viruses and mock-infected control, at day 5 p.i. MHV was detected by immunolabeling with a MAb against the N protein of MHV as described in the text. Viral antigen always colocalized with necrotic areas. No signs of viral antigen were found in a mock-infected control. Magnification, ×100.

performed virus stability studies, but we have observed that in cell culture recombinant H716D viruses exhibited similar levels of cell-associated virus compared to WT A59, but highly reduced levels of virus released (Fig. 2). This result might suggest that H716D virus is less stable than WT A59. Curiously, H716D virus is found in the brain after i.h. inoculation (Fig. 5). We have observed this phenomena with hr2 parental and recombinant viruses (Rhr2-A and -B), as well as other highly hepatotropic viruses (MHV-2 and Penn-98) (data not shown). These findings do not contradict the fact that in general, mice do not develop CNS disease after i.h. inoculation. Rather it reflects the fact that mice inoculated with highly hepatotropic viruses directly into the liver, succumb to infection shortly after inoculation (2 to 6 days, depending on virus strain). Consequently, at 5 days p.i. (peak of virus replication) mice are usually moribund and blood-brain barrier is likely damaged allowing virus entry into the CNS.

Our findings suggest that conformation of the spike is a key determinant of pathogenesis. A complicating factor in the interpretation of our data is that no crystal structure has been determined for the S protein of any coronavirus. However, by comparison with other class I viral fusion glycoprotein's, murine coronavirus spike proteins consist of an N-terminal receptor binding domain within the S1 subunit followed by an exposed protease cleavage site, a fusion domain containing several heptad repeats, and transmembrane and cytoplasm domains, all within the S2 subunit (5, 6, 15). Domains responsible for the receptor binding activity of some coronaviruses have been identified (7, 54, 56, 57). In the case of MHV, amino acids 1–330 of S comprise the minimal RBD for virus receptor in vitro and in vivo (29, 52). The Q159L substitution, which maps in the RBD domain of S, seems to play a key role in determining the lack of hepatotropism in vivo. Curiously, the Q159L substitution does not affect the phenotype in the brain nor the in vitro replication kinetics compared to WT A59. This may reflect differences in the interaction of S with the receptor in the liver versus the brain. Murine CEACAM1a (a member of the carcinoembryonic antigen family of cell adhesion molecules) is the main virus receptor. The mouse genome contains two CEACAM-like genes (CEACAM1 and CEACAM2) and murine CEACAM1 is expressed as allelic glycoproteins (CEACAM1a and CEACAM1b). Hemmila et al. (21) have recently generated two mouse strains that have a complete ablation of the CEACAM1a proteins. These CEACAM1a$^{-/-}$ mice are fully resistant to MHV-A59 infection, suggesting that CEACAM1a is the only receptor for MHV-A59 in C57BL/6 mice. Taking together, it seems likely that MHV may interact in the liver with still undefined coreceptors. Ontiveros et al. (40)., have recently demonstrated that a serine-to-glycine change at position 310 of the neurotropic JHM strain spike is associated with increased lateral spread in the CNS, higher viral load and neurovirulence. Although S310G was not isolated in vivo, these results highlight that the putative RBD is also a determinant of neuropathogenesis.

All three revertants isolated after in vivo adaptation in the liver of mice contained the same amino acid substitution E1035D in the heptad repeat domain 1 (Fig. 1; Table 1). We have compared the S sequences obtained after in vivo adaptation to published S sequences of other MHV strains (MHV-2, MHV-3, MHV-JHM, MHV-4, MHV-S) (data not shown). It is intriguing that all of these MHV strains sequences that we have analyzed contain aspartic acid (D) at position 1035, whereas MHV-A59 strain has glutamic acid (E). Thus, E1035D is an amino acid substitution in the context of the A59 strain, but it is WT compared with other MHV strains. Although recombinant viruses with the E1035D substitution alone exhibit a WT A59-like phenotype, our results also demonstrate that the E1035D substitution may overcome the lack of hepatotropism induced by Q159L (Fig. 4 and 6). It is likely that the heptad repeat domain E1035D amino acid substitution, albeit a conservative change, may compensate for Q159L in S1 by affecting the conformation of S. In support of this suggestion, Grosse and Sidell (18), have reported that monoclonal antibody (MAb)-resistant mutants of a MAb with specificity for an epitope in S1 had point mutations which mapped adjacent to the second heptad repeat domain. This may also suggest that the proper spatial arrangement of the S1 and S2 subunits is crucial for the biologic functions of the S protein. In addition, we have also demonstrated that the RBD and the rest of the spike must coevolve to optimize function in viral entry and spread (55).

The R654H substitution maps in a region of S in which functional domains have not been yet identified. It is intriguing that whereas R654H alone exhibited a WT A59-like phenotype, and did not affect the lack of hepatotropism caused by Q159L (recombinant virus Q159L-R654H had the same phenotype as Q159L), in the context of Q159L-H716D it was able to overcome the nonhepatotropic phenotype of Q159L-H716D virus to levels somewhat intermediate between A59 and hr2 viruses.

The relationship between cleavage and fusion differs among coronaviruses, and even among MHV strains. Spike-induced cell-cell fusion does not have an absolute requirement for cleavage of S. For MHV-A59, the kinetics of fusion of infected cells is enhanced by cleavage of the spike protein (5, 51). In cell culture, the amino acid substitution in the cleavage site of A59 spike (H716D) reduce (but never completely prevented) the amount of S protein cleavage compared to WT A59 spike (10, 24). We have reported a lack of cleavage of WT MHV-A59 strain spike protein in virions present in liver homogenates of infected C57BL/6 mice (25); in contrast, in continuously cultured L2 cells A59 spike is cleaved (17). This finding suggested that in the liver, spike-mediated cell fusion may not play a role in virulence. In addition, we have recently demonstrated that there is no correlation between ability to induce cell-to-cell fusion in vitro and ability to cause disease in vivo (24). The process by which viruses spread from cell to cell may be mechanistically different from virus entry into cells, and may require the presence of different cellular surface molecules. It remains to be experimentally determined why the H716D substitution that reduced S cleavage in cell culture causing a fusion-delayed phenotype, correlates with lethal hepatitis, higher viral load and enhanced virus spread in the liver of infected mice.

Like other RNA viruses, coronaviruses exhibit a high potential for variation and adaptation, which is reflected in their serological diversity and capacity to produce persistent infections in host animals as well as in cell culture (3, 8, 47, 49). It was well accepted that coronaviruses exhibit a narrow host range that is determined by the spike protein (26–28, 46, 53). Expression of the receptor of MHV in cells of heterologous,

nonpermissive species (such as human (HeLa) and hamster (BHK cells) renders them permissive to infection (12). A change of receptor utilization may be associated with the transition or enhancement in host range of coronaviruses from one species to the other. The origin of SARS-CoV remains unknown. A prominent hypothesis is that SARS-CoV may have a reservoir in another species and have jumped into humans (13). It has been recently reported that the genomes of viruses isolated from civet cats are close in sequence to human isolates (19). Comparison between human and civet cat virus isolates indicates 10 consistent amino acid changes in the spike protein of human and animal isolates (19). Among the differences there are two amino acids substitutions in the heptad repeat domain regions of S (19). Experimental interspecies transfer of MHV was associated with altered receptor usage (3, 22). It has been previously shown that MHV can evolve through high passage persistent infection in tissue culture to have an expanded host range (2, 3, 45, 47). This expanded host range was associated with various amino acids substitutions in the spike protein (46, 53). In order to assess whether the highly virulent hr2 isolate may exhibit expanded host range, we performed in vitro infections of human embryonic kidney cell (293T), human ovarian carcinoma (HeLa), feline whole fetus (FCWF), and baby hamster kidney BHK-21 cells. These cells are known to lack the MHV receptor (mCEACAM1). These experiments (data not shown), suggested that the hr2 isolate was not able to infect cells lacking the mCEACAM molecule (at least in the cells tested), and in addition, that hr2 does not have the ability to exploit other surface molecules present in these particular cells to initiate infection.

Multiple types of genetic modifications may result in alterations of virus cell tropism and virulence, leading to broad host range and differences in pathogenesis (48). Despite the quasispecies nature of RNA viruses, tolerable changes in the viral envelope proteins are constrained by the need to interact with a certain receptor (1). Single amino acid substitutions in surface or capsid viral proteins have been identified to affect receptor recognition, cellular tropism, and pathogenesis. We as well as may others have previously addressed the role of the spike in coronavirus pathogenesis (reviewed in references 38 and 39). To our knowledge, our findings demonstrate for the first time that coronaviruses may rapidly evolve in vivo into lethal phenotypes by functional compensation of a detrimental amino acid substitution in the receptor binding domain of the Spike glycoprotein.

ACKNOWLEDGMENTS

This work was supported by NIH grant AI 17418 and AI60021 (formerly NS-21954).

We are grateful to Paul Masters for the donor plasmid pMH54 and the helper virus fMHV and Julian Leibowitz for providing MAb clone 1-16-1.

REFERENCES

1. **Baranowski, E., C. M. Ruiz-Jarabo, and E. Domingo.** 2001. Evolution of cell recognition by viruses. Science **292:**1102–1105.
2. **Baric, R. S., G. W. Nelson, J. O. Fleming, R. J. Deans, J. G. Keck, N. Casteel, and S. A. Stohlman.** 1988. Interactions between coronavirus nucleocapsid protein and viral RNAs: implications for viral transcription. J. Virol. **62:** 4280–4287.
3. **Baric, R. S., E. Sullivan, L. Hensley, B. Yount, and W. Chen.** 1999. Persistent infection promotes cross-species transmissibility of mouse hepatitis virus. J. Virol. **73:**638–649.
4. **Batts, K. P., and J. Ludwig.** 1995. Chronic hepatitis. An update on terminology and reporting. Am. J. Surg. Pathol. **19:**1409–1417.
5. **Bos, E. C., L. Heijnen, W. Luytjes, and W. J. Spaan.** 1995. Mutational analysis of the murine coronavirus spike protein: effect on cell-to-cell fusion. Virology **214:**453–463.
6. **Bosch, B. J., R. van der Zee, C. A. de Haan, and P. J. Rottier.** 2003. The coronavirus spike protein is a class I virus fusion protein: structural and functional characterization of the fusion core complex. J. Virol. **77:**8801–8811.
7. **Breslin, J. J., I. Mork, M. K. Smith, L. K. Vogel, E. M. Hemmila, A. Bonavia, P. J. Talbot, H. Sjostrom, O. Noren, and K. V. Holmes.** 2003. Human coronavirus 229E: receptor binding domain and neutralization by soluble receptor at 37°C. J. Virol. **77:**4435–4438.
8. **Chen, W., and R. S. Baric.** 1996. Molecular anatomy of mouse hepatitis virus persistence: coevolution of increased host cell resistance and virus virulence. J. Virol. **70:**3947–3960.
9. **Das Sarma, J., L. Fu, J. C. Tsai, S. R. Weiss, and E. Lavi.** 2000. Demyelination determinants map to the spike glycoprotein gene of coronavirus mouse hepatitis virus. J. Virol. **74:**9206–9213.
10. **de Haan, C. A., K. Stadler, G. J. Godeke, B. J. Bosch, and P. J. Rottier.** 2004. Cleavage inhibition of the murine coronavirus spike protein by a furin-like enzyme affects cell-cell but not virus-cell fusion. J. Virol. **78:**6048–6054.
11. **Drosten, C., S. Gunther, W. Preiser, S. van der Werf, H. R. Brodt, S. Becker, H. Rabenau, M. Panning, L. Kolesnikova, R. A. Fouchier, A. Berger, A. M. Burguiere, J. Cinatl, M. Eickmann, N. Escriou, K. Grywna, S. Kramme, J. C. Manuguerra, S. Muller, V. Rickerts, M. Sturmer, S. Vieth, H. D. Klenk, A. D. Osterhaus, H. Schmitz, and H. W. Doerr.** 2003. Identification of a novel coronavirus in patients with severe acute respiratory syndrome. N. Engl. J. Med. **348:**1967–1976.
12. **Dveksler, G. S., S. E. Gagneten, C. A. Scanga, C. B. Cardellichio, and K. V. Holmes.** 1996. Expression of the recombinant anchorless N-terminal domain of mouse hepatitis virus (MHV) receptor makes hamster of human cells susceptible to MHV infection. J. Virol. **70:**4142–4145.
13. **Enserink, M.** 2003. Infectious diseases. Clues to the animal origins of SARS. Science **300:**1351.
14. **Frana, M. F., J. N. Behnke, L. S. Sturman, and K. V. Holmes.** 1985. Proteolytic cleavage of the E2 glycoprotein of murine coronavirus: host-dependent differences in proteolytic cleavage and cell fusion. J. Virol. **56:**912–920.
15. **Gallagher, T. M., and M. J. Buchmeier.** 2001. Coronavirus spike proteins in viral entry and pathogenesis. Virology **279:**371–374.
16. **Gallagher, T. M., S. E. Parker, and M. J. Buchmeier.** 1990. Neutralization-resistant variants of a neurotropic coronavirus are generated by deletions within the amino-terminal half of the spike glycoprotein. J. Virol. **64:**731–741.
17. **Gombold, J. L., S. T. Hingley, and S. R. Weiss.** 1993. Fusion-defective mutants of mouse hepatitis virus A59 contain a mutation in the spike protein cleavage signal. J. Virol. **67:**4504–4512.
18. **Grosse, B., and S. G. Siddell.** 1994. Single amino acid changes in the S2 subunit of the MHV surface glycoprotein confer resistance to neutralization by S1 subunit-specific monoclonal antibody. Virology **202:**814–824.
19. **Guan, Y., B. J. Zheng, Y. Q. He, X. L. Liu, Z. X. Zhuang, C. L. Cheung, S. W. Luo, P. H. Li, L. J. Zhang, Y. J. Guan, K. M. Butt, K. L. Wong, K. W. Chan, W. Lim, K. F. Shortridge, K. Y. Yuen, J. S. Peiris, and L. L. Poon.** 2003. Isolation and characterization of viruses related to the SARS coronavirus from animals in southern China. Science **302:**276–278.
20. **Haring, J., and S. Perlman.** 2001. Mouse hepatitis virus. Curr. Opin. Microbiol. **4:**462–466.
21. **Hemmila, E., C. Turbide, M. Olson, S. Jothy, K. V. Holmes, and N. Beauchemin.** 2004. Ceacam1a$^{-/-}$ mice are completely resistant to infection by murine coronavirus mouse hepatitis virus A59. J. Virol. **78:**10156–10165.
22. **Hensley, L. E., K. V. Holmes, N. Beauchemin, and R. S. Baric.** 1998. Virus-receptor interactions and interspecies transfer of a mouse hepatitis virus. Adv. Exp. Med. Biol. **440:**33–41.
23. **Hingley, S. T., J. L. Gombold, E. Lavi, and S. R. Weiss.** 1994. MHV-A59 fusion mutants are attenuated and display altered hepatotropism. Virology **200:**1–10.
24. **Hingley, S. T., I. Leparc-Goffart, S. H. Seo, J. C. Tsai, and S. R. Weiss.** 2002. The virulence of mouse hepatitis virus strain A59 is not dependent on efficient spike protein cleavage and cell-to-cell fusion. J. Neurovirol. **8:**400–410.
25. **Hingley, S. T., I. Leparc-Goffart, and S. R. Weiss.** 1998. The spike protein of murine coronavirus mouse hepatitis virus strain A59 is not cleaved in primary glial cells and primary hepatocytes. J. Virol. **72:**1606–1609.
26. **Holmes, K. V.** 1996. Coronaviridae: the viruses and their replication., p. 1075–1103. *In* B.N. Fields, D. M. Knipe, and P. M. Howley (ed.), Fields virology, 3rd ed. Lippincott-Raven Publishers, Philadelphia, Pa.
27. **Holmes, K. V., D. B. Tresnan, and B. D. Zelus.** 1997. Virus-receptor interactions in the enteric tract. Virus-receptor interactions. Adv. Exp. Med. Biol. **412:**125–133.
28. **Holmes, K. V., B. D. Zelus, J. H. Schickli, and S. R. Weiss.** 2001. Receptor specificity and receptor-induced conformational changes in mouse hepatitis virus spike glycoprotein. Adv. Exp. Med. Biol. **494:**173–181.

29. **Kubo, H., Y. K. Yamada, and F. Taguchi.** 1994. Localization of neutralizing epitopes and the receptor-binding site within the amino-terminal 330 amino acids of the murine coronavirus spike protein. J. Virol. **68:**5403–5410.
30. **Kuo, L., G. J. Godeke, M. J. Raamsman, P. S. Masters, and P. J. Rottier.** 2000. Retargeting of coronavirus by substitution of the spike glycoprotein ectodomain: crossing the host cell species barrier. J. Virol. **74:**1393–1406.
31. **Lavi, E., D. H. Gilden, M. K. Highkin, and S. R. Weiss.** 1986. The organ tropism of mouse hepatitis virus A59 in mice is dependent on dose and route of inoculation. Lab. Anim. Sci. **36:**130–135.
32. **Lavi, E., D. H. Gilden, Z. Wroblewska, L. B. Rorke, and S. R. Weiss.** 1984. Experimental demyelination produced by the A59 strain of mouse hepatitis virus. Neurology **34:**597–603.
33. **Leparc-Goffart, I., S. T. Hingley, M. M. Chua, X. Jiang, E. Lavi, and S. R. Weiss.** 1997. Altered pathogenesis of a mutant of the murine coronavirus MHV-A59 is associated with a Q159L amino acid substitution in the spike protein. Virology **239:**1–10.
34. **Leparc-Goffart, I., S. T. Hingley, M. M. Chua, J. Phillips, E. Lavi, and S. R. Weiss.** 1998. Targeted recombination within the spike gene of murine coronavirus mouse hepatitis virus-A59: Q159 is a determinant of hepatotropism. J. Virol. **72:**9628–9636.
35. **Navas, S., S. H. Seo, M. M. Chua, J. Das Sarma, S. T. Hingley, E. Lavi, and S. R. Weiss.** 2001. Role of the spike protein in murine coronavirus induced hepatitis: an in vivo study using targeted RNA recombination. Adv. Exp. Med. Biol. **494:**139–144.
36. **Navas, S., S. H. Seo, M. M. Chua, J. D. Sarma, E. Lavi, S. T. Hingley, and S. R. Weiss.** 2001. Murine coronavirus spike protein determines the ability of the virus to replicate in the liver and cause hepatitis. J. Virol. **75:**2452–2457.
37. **Navas, S., and S. R. Weiss.** 2003. Murine coronavirus-induced hepatitis: JHM genetic background eliminates A59 spike-determined hepatotropism. J. Virol. **77:**4972–4978.
38. **Navas-Martin, S., and S. R. Weiss.** 2004. Coronavirus replication and pathogenesis: Implications for the recent outbreak of severe acute respiratory syndrome (SARS), and the challenge for vaccine development. J. Neurovirol. **10:**75–85.
39. **Navas-Martin, S., and S. R. Weiss.** 2003. SARS:Lessons learned from other coronaviruses. Viral Immunol. **16:**461–474.
40. **Ontiveros, E., T. S. Kim, T. M. Gallagher, and S. Perlman.** 2003. Enhanced virulence mediated by the murine coronavirus, mouse hepatitis virus strain JHM, is associated with a glycine at residue 310 of the spike glycoprotein. J. Virol. **77:**10260–10269.
41. **Peiris, J. S., S. T. Lai, L. L. Poon, Y. Guan, L. Y. Yam, W. Lim, J. Nicholls, W. K. Yee, W. W. Yan, M. T. Cheung, V. C. Cheng, K. H. Chan, D. N. Tsang, R. W. Yung, T. K. Ng, and K. Y. Yuen.** 2003. Coronavirus as a possible cause of severe acute respiratory syndrome. Lancet **361:**1319–1325.
42. **Phillips, J. J., M. M. Chua, E. Lavi, and S. R. Weiss.** 1999. Pathogenesis of chimeric MHV4/MHV-A59 recombinant viruses: the murine coronavirus spike protein is a major determinant of neurovirulence. J. Virol. **73:**7752–7760.
43. **Reed, L. J., and H. Muench.** 1938. A simple method of estimating fifty per cent points. Am. J. Hyg. **27:**493–497.
44. **Ricard, C. S., and L. S. Sturman.** 1985. Isolation of the subunits of the coronavirus envelope glycoprotein E2 by hydroxyapatite high-performance liquid chromatography. J. Chromatogr. **326:**191–197.
45. **Sawicki, S. G., J. H. Lu, and K. V. Holmes.** 1995. Persistent infection of cultured cells with mouse hepatitis virus (MHV) results from the epigenetic expression of the MHV receptor. J. Virol. **69:**5535–5543.
46. **Schickli, J. H., L. B. Thackray, S. G. Sawicki, and K. V. Holmes.** 2004. The N-terminal region of the murine coronavirus spike glycoprotein is associated with the extended host range of viruses from persistently infected murine cells. J. Virol. **78:**9073–9083.
47. **Schickli, J. H., B. D. Zelus, D. E. Wentworth, S. G. Sawicki, and K. V. Holmes.** 1997. The murine coronavirus mouse hepatitis virus strain A59 from persistently infected murine cells exhibits an extended host range. J. Virol. **71:**9499–9507.
48. **Schneider-Schaulies, J.** 2000. Cellular receptors for viruses: links to tropism and pathogenesis. J. Gen. Virol. **81:**1413–1429.
49. **Sidell, S. G.** 1995. The coronaviridae. Plenum Press, New York, N.Y.
50. **Spaan, W., D. Cavanagh, and M. C. Horzinek.** 1988. Coronaviruses: structure and genome expression. J. Gen. Virol. **69:**2939–2952.
51. **Stauber, R., M. Pfleiderera, and S. Siddell.** 1993. Proteolytic cleavage of the murine coronavirus surface glycoprotein is not required for fusion activity. J. Gen. Virol. **74:**183–191.
52. **Suzuki, H., and F. Taguchi.** 1996. Analysis of the receptor-binding site of murine coronavirus spike protein. J. Virol. **70:**2632–2636.
53. **Thackray, L. B., and K. V. Holmes.** 2004. Amino acid substitutions and an insertion in the spike glycoprotein extend the host range of the murine coronavirus MHV-A59. Virology **324:**510–524.
54. **Tresnan, D. B., R. Levis, and K. V. Holmes.** 1996. Feline aminopeptidase N serves as a receptor for feline, canine, porcine, and human coronaviruses in serogroup I. J. Virol. **70:**8669–8674.
55. **Tsai, J. C., B. D. Zelus, K. V. Holmes, and S. R. Weiss.** 2003. The N-terminal domain of the murine coronavirus spike glycoprotein determines the CEACAM1 receptor specificity of the virus strain. J. Virol. **77:**841–850.
56. **Wentworth, D. E., and K. V. Holmes.** 2001. Molecular determinants of species specificity in the coronavirus receptor aminopeptidase N (CD13): influence of N-linked glycosylation. J. Virol. **75:**9741–9752.
57. **Yeager, C. L., R. A. Ashmun, R. K. Williams, C. B. Cardellichio, L. H. Shapiro, A. T. Look, and K. V. Holmes.** 1992. Hum. aminopeptidase N is a receptor for human coronavirus 229E. Nature **357:**420–422.